(Pietschmann et al., 2002). The HCV RNA level in RCYM1 cells was approximately 5×10^6 copies/μg total RNA as determined by real-time reverse transcriptase-polymerase chain reaction (RT-PCR). The expression and subcellular localization of HCV protein were confirmed by Western blotting and immunofluorescence analysis (data not shown). To develop 3D RFB cultures, first we loaded RCYM1 cells onto an RFB column by flowing cell suspension, after which the cells were attached to carrier beads. Cells proliferated within the 3D matrix, and culture medium was circulated radially through the column.

In order to investigate whether HCV-like particles (HCV-LPs) were secreted from RCYM1 cells in the RFB culture system, we fractionated culture fluid collected after 5–10 days of culture by continuous 10–60% (wt/vol) sucrose density gradient centrifugation. HCV RNA and core protein were predominantly detected in the 1.15–1.20 g/ml fractions, with maximal detection in the 1.18 g/ml fraction (Figs. 1A and B). In the same experiment using 5–15 cells, in which a subgenomic HCV replicon replicates, no peak similar to that observed in RCYM1 cells corresponding to HCV RNA was detected. In both RCYM1 cells and 5–15 cells in the RFB culture system, a substantial amount of HCV RNA was detected in the 1.03–1.07 g/ml fractions (Fig. 1A). Consistent with a previous report by Pietschmann et al. (2002), these RNAs released from cells with a subgenomic replicon did not correspond to virus particles. When an equivalent number of RCYM1 cells were cultured in a monolayer culture system, limited amounts of HCV RNA and core protein were detected in the culture supernatant (Figs. 1A and B).

The mature HCV virion is thought to have a nucleocapsid and an outer envelope composed of a lipid membrane with viral envelope glycoproteins. Culture fluids were treated with NP40 in order to solubilize lipids and were then subjected to sucrose density gradient centrifugation. HCV RNA sedimented to a density of 1.22 g/ml rather than 1.18 g/ml (Fig. 1C), indicating that the density of HCV particles became higher due to de-envelopment. Transmission electron microscopy (TEM) of the 1.18 g/ml fraction, which was subjected to negative staining after concentration, revealed particle structures with diameters of 30–60 nm and a major particle size of 50 nm (Fig. 1D). No similar particle-like structures were observed in the same density fraction of the RCYM1 monolayer culture (Fig. 1E) or in the 1.23 g/ml fraction of the RCYM1-RFB culture (data not shown). These results indicate that, in the RFB system, the production and secretion of HCV-LPs is possible with a selectable dicistronic HCV genome.

Production and secretion of HCV-LPs from spheroid culture of RCYM1 cells using TGP

In the 3D RFB culture system for RCYM1 cells, extracellular secretion of HCV-LPs was observed. Based on this observation, we hypothesized that morphological changes occurring in 3D culture, such as polarity formation, promote advantageous in the assembly of viral proteins, particle formation, and extracellular secretion. To examine whether similar phenomena could be observed in other 3D culture systems, we investigated HCV-LP expression using a 3D culture system with TGP as a carrier.

TGP is a biocompatible polymer made from conjugates of polyethyleneglycol and poly-*N*-isopropylacrylamide, which is a thermoresponsive polymer composed of *N*-isopropylacrylamide and *n*-butylmethacrylate. The TGP solution possesses sol-gel transition properties; it is water soluble (sol phase) at temperatures below the transition temperature, and it is insoluble (gel phase) above it. It is possible to manipulate the transition temperatures through molecular engineering. The transition temperature for TGP in the present experiments was approximately 20 °C.

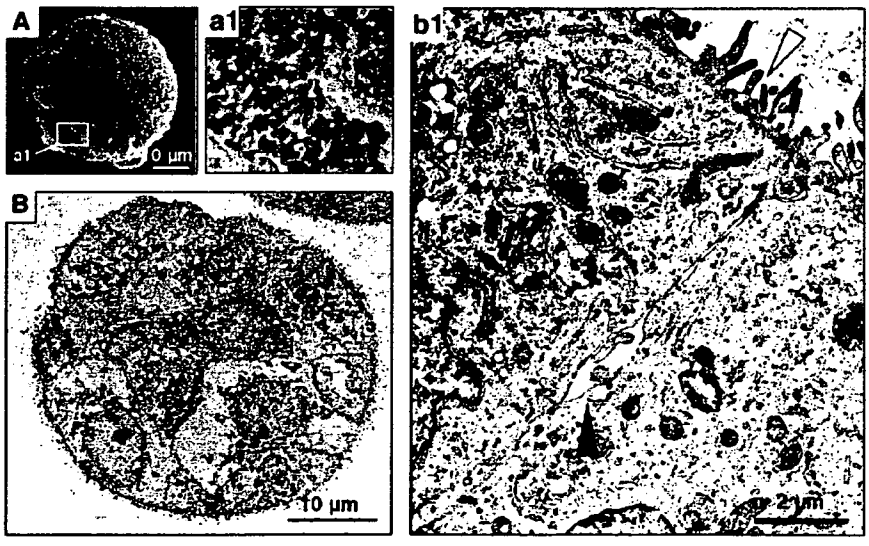

Fig. 2. Huh-7 and RCYM1 cells form spheroids in thermoreversible gelation polymer (TGP). Scanning electron microscopy (A and a1) and transmission electron microscopy (B and b1) of RCYM1 cells cultured in TGP for 8 days. Open arrowhead, microvilli; closed arrowheads, bile canaliculi-like structures.

RCYM1 cells, which were seeded into the TGP, formed three-dimensional compacted aggregates called spheroids after 3 days of culture, and numerous spheroids with diameters of approximately 1 mm were observed after 7–10 days of culture. After 8 days of culture, the spheroids were fixed and examined by scanning electron microscopy (Figs. 2A and a1) and ultrathin sections were examined by TEM (Figs. 2B and b1). Well-developed microvilli, a feature of polarized epithelium, were observed on the cell surface (Figs. 2A and a1). Bile canaliculi-like structures were also observed within intercellular spaces, and they appeared to be connected via tight junctions (Figs. 2B and b1). This cytomorphology, similar to that observed in the RFB culture (Kawada et al., 1998; Matsuura et al., 1998), correlated well with the features of mature liver tissue.

It is known that the replication of HCV replicons in Huh-7 cells depends on host cell growth. We found that the growth of RCYM1 cells in the TGP culture system was significantly slower than that of cells in monolayer culture (Fig. 3A). Accordingly, the expression of HCV proteins (Fig. 3B) in the RCYM1 spheroids was apparently lower compared to those observed in the monolayer cells. The viral RNA copy number in the spheroids was approximately one tenth of that in the monolayer culture (data not shown). The results of sucrose density gradient analysis of culture supernatant demonstrated co-sedimentation of HCV RNAs and core proteins at a density of 1.15–1.20 g/ml, with a peak at 1.18 g/ml (Figs. 3C and D). This distribution was consistent with the pattern obtained in RFB culture (Figs. 1A and B). It should be noted that in these experiments, lower cell numbers were used in the 3D cultures than in the monolayer cultures because of the slower growth of cells. As estimated from the quantitative data of the 1.15–1.20 g/ml fractions of the culture supernatants, 0.1–1 copies of HCV RNA/cell/day are produced and assembled into viral particles in the TGP-cultured RCYM1 cells.

TEM analysis of the 1.18 g/ml fraction after negative staining showed particle structures with a diameter of 50–60 nm and spike-like projections (Fig. 3E). Observation of ultrathin sections indicated a lipid bilayer-like membrane structure with a

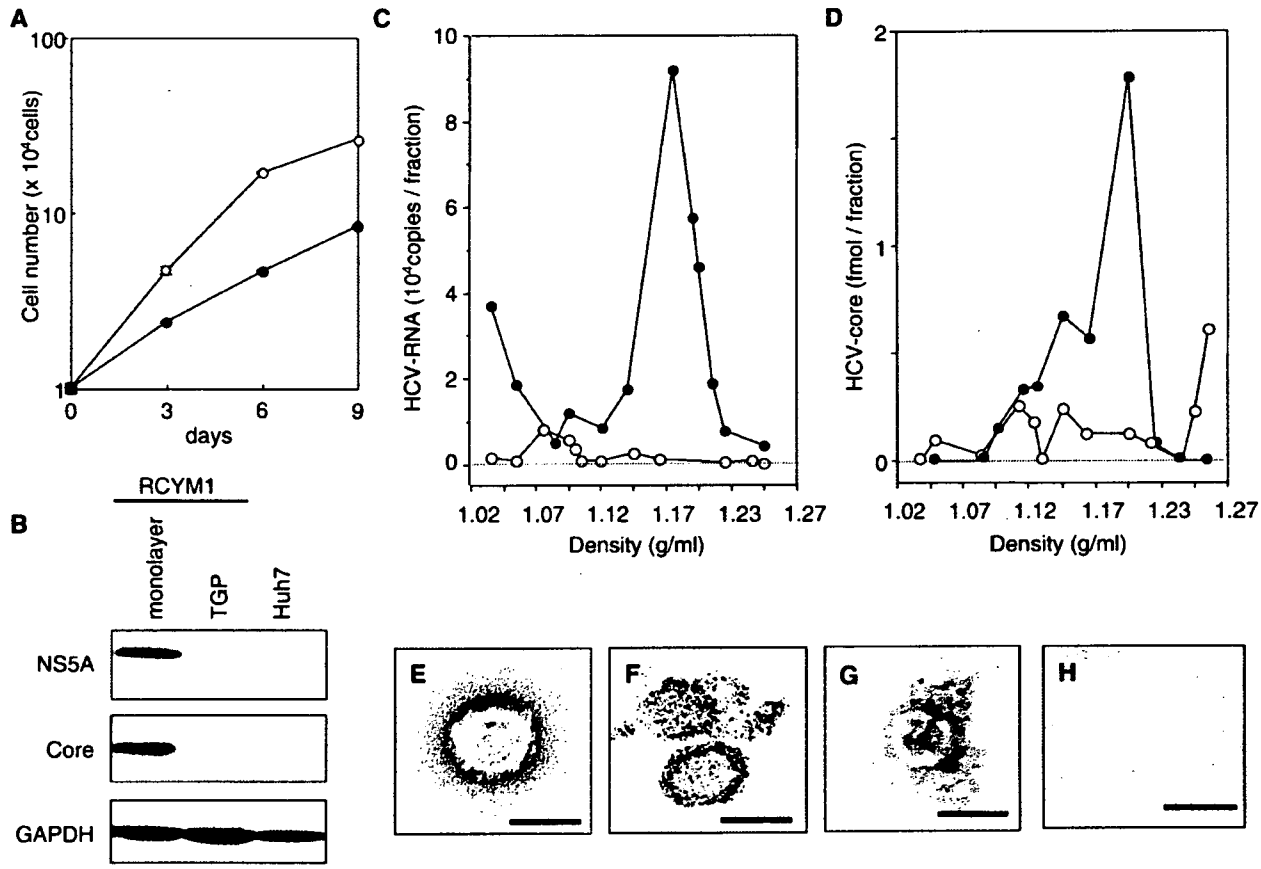

Fig. 3. Expression of HCV proteins in RCYM1 cells and secretion of viral particles in TGP culture. (A) Cell growth curves of the TGP (closed circles) and monolayer (open circles) culture of RCYM1 cells. Cells were harvested at days 0, 3, 6, and 9 postinoculation and cell numbers were determined. (B) Western blotting of HCV core and NS5A proteins in RCYM1 cells and control Huh-7 cells. (C, D) Sucrose density gradient analysis of culture supernatants of RCYM1 cells. The culture supernatants were fractionated as described in Materials and methods. HCV RNA (C) and core protein (D) in each fraction were determined by ELISA and real-time RT-PCR, respectively. Representative data from three independent experiments are shown. Closed circles, TGP culture; open circles, monolayer culture. (E–H) Electron microscopy of HCV-like particles (HCV-LPs) in the supernatants of TGP-cultured RCYM1 cells. (E) Negative staining of HCV-LPs in the 1.18 g/ml density fraction. There was no spherical structure in 1.05 g/ml density fraction, as shown in panel H. (F) Ultrathin section of HCV-LPs. Precipitated HCV-LP samples were prepared from the 1.18 g/ml fraction as described in Materials and methods. (G) Immunogold labeling of HCV-LPs with an anti-E2 antibody in the 1.18 g/ml density fraction. Gold particles, 5 nm; scale bars, 50 nm.

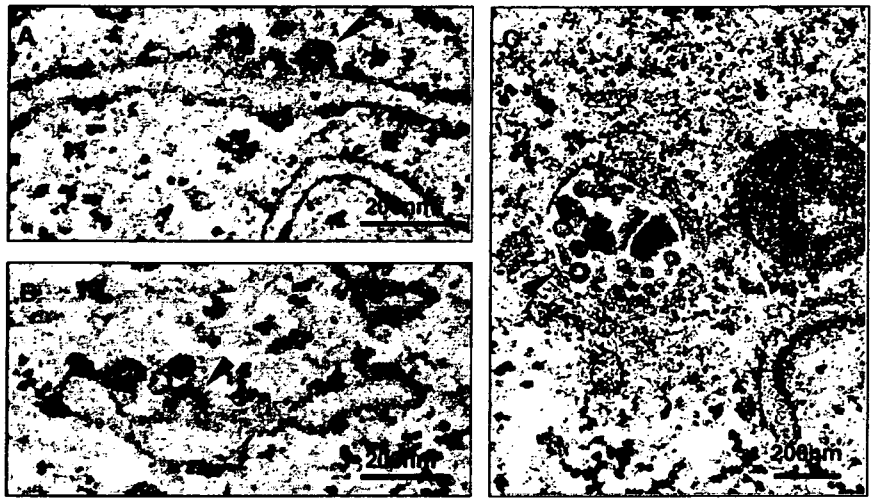

Fig. 4. Electron microscopy of ultrathin sections of RCYM1 cells grown in TGP. HCV-LPs in TGP-cultured RCYM1 cells. Spherical virus-like particles 50–60 nm in diameter (arrowheads) were observed at the ER membranes (A, B) and in the cytoplasmic vesicles (C).

width of approximately 5 nm (Fig. 3F). Immunoelectron microscopic study using anti-E2 antibody revealed HCV envelope protein(s) on the particle surface (Fig. 3G). Substantial amounts of HCV RNA were detected in the 1.03–1.05 g/ml fractions of the supernatant (Fig. 3C); however, HCV-LP structures were not observed in these fractions (Fig. 3H). These results were consistent with those from the RFB system, as shown above. The efficacy of 3D cell culture systems in virion formation was thus demonstrated in both the RFB and TGP culture systems using human liver-derived cells.

Ultrastructural localization of HCV-LPs in TGP-cultured spheroids of RCYM1 cells

We next determined the intracellular localization of HCV-LPs produced in RCYM1-TGP culture at the ultrastructural level by electron microscopic (EM) analysis of ultrathin sections. Spherical particles having membrane-like structures with short surface projections (diameter, 50–60 nm) were observed primarily at the endoplasmic reticulum (ER) membrane (Fig. 4A) as well as in the dilated cisternae of the ER (Fig. 4B). In vesicles, these virus-like particles were frequently associated with amorphous materials (Fig. 4C). In a previous study, Shimizu et al. (1996) report that virus-like particles with similar morphology and size were observed in human B cells infected with HCV. No similar particle-like structures were observed in RCYM1 cells in monolayer culture or in subgenomic replicon 5–15 in cells in TGP culture (data not shown).

In order to determine whether the virus-like particles observed by conventional TEM in the present experiment were HCV-LPs, we conducted immunoelectron microscopic analysis with anti-core antibody and anti-E1 antibody. Double-labeling experiments showed that the virus-like particles associated with the ER membrane exhibited immunoreactivity for both HCV proteins, and that the E1 protein surrounded the core proteins (Fig. 5A). To the best of our knowledge, this is the first report to clearly demonstrate that the viral envelope protein surrounds the core protein in HCV particle formation. As a negative control, thin sections prepared from subgenomic RNA containing 5–15 cells were stained with these antibodies and were found to exhibit negligible levels of background immunostaining (data not shown).

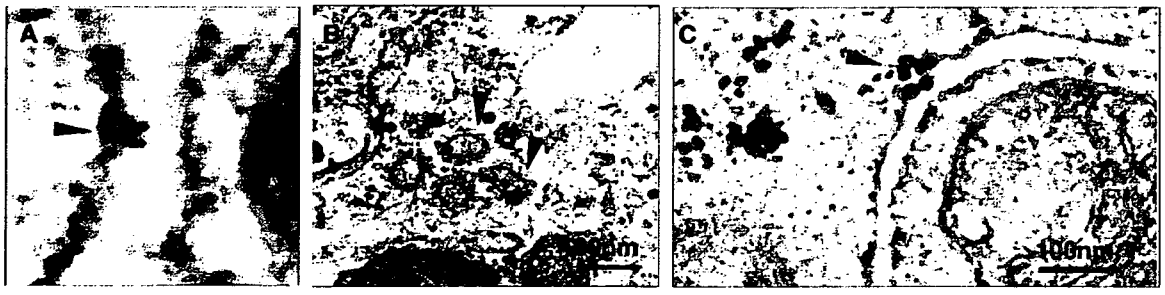

Fig. 5. Immunoelectron microscopy of ultrathin sections of TGP-cultured RCYM1 cells. (A) Double immunostaining with anti-E1 and anti-core monoclonal antibodies. Core protein-specific gold particles (10 nm in diameter) and E1 protein-specific gold particles (5 nm in diameter) formed rosettes on the surface of the ER membrane. (B and C) Silver-intensified immunogold staining with anti-core (B) and anti-E1 (C) antibodies. The second antibody conjugated with gold particles 1.4 nm in diameter was applied, followed by enlargement of the particles by the silver enhancement reagent. Arrowheads indicate virus-like particles reacting with anti-core and/or anti-E1 antibodies.

It is generally difficult to visualize intracellular microstructures and perform antigenic protein localizations using immunogold electron microscopy due to the low resolution and contrast of micrographs. In order to overcome this difficulty, we applied a silver-intensified immunogold labeling method in our experiment (Figs. 5B and C). Using this method, antigen-reactive immunogold particles approximately 20 nm in diameter were observed. Specific immunolabeling of core and E1 protein was detected in the ER or on the ER membranes. Intense immunopositive reactions were also seen on the virus-like particles observed in cytoplasmic vesicles and on ER membranes; however, no such immunolabeling was observed when normal mouse serum was used as a first antibody (data not shown). These results confirm the ultrastructural observations of conventional TEM and suggest that the formation of HCV particles is achieved by budding of the putative core particles at the ER membrane.

Infectivity of HCV-LPs depends on E2 glycoprotein

To determine whether HCV-LPs released from RCYM1 cells cultured in the TGP system are infectious, we inoculated naive Huh-7.5.1 cells (Zhong et al., 2005), which are HCV-negative Huh-7.5 (Blight et al., 2002)-derived cells, with a culture supernatant of RCYM1 spheroids. HCV RNAs in the cells at days 0, 1, 2, 3, and 7 postinoculation were determined by real-time RT-PCR. Fig. 6A shows the kinetics of HCV RNA after the inoculation of HCV-LPs. HCV RNA levels in the infected Huh-7.5.1 cells fluctuated at the indicated times, reaching 10^3–10^4 copies/μg of cellular RNA at days 1–7. Immunofluorescence staining 4 days postinoculation revealed that approximately 1% of cells were positive for NS5A protein (Fig. 6B). In contrast, no NS5A-positive cells were detected when the cell supernatant sample obtained from 5 to 15 cell cultured in TGP was used to inoculate Huh-7.5.1 cells (data not shown). These results suggest that HCV-LPs released from TGP-cultured RCYM1 cells are infectious.

To further determine whether viral envelope proteins mediate infection by HCV-LPs, we preincubated HCV-LPs with the anti-E2 monoclonal antibody AP33, which demonstrates potent neutralization of infectivity against HCV pseudoparticles carrying E1 and E2 proteins representative of the major genotypes 1 through 6 (Owsianka et al., 2005), or with patient sera with high titers of HCV neutralization of binding (NOB) antibodies (Ishii et al., 1998), or with anti-FLAG antibody (Fig. 6C). NOB antibodies have the ability to neutralize the binding of E2 protein to human cells (Rosa et al., 1996), and NOB3 and NOB4 were sera obtained from patients who recovered naturally from chronic hepatitis C (Ishii et al., 1998). Intracellular HCV RNA levels were decreased by 43%, 28%,

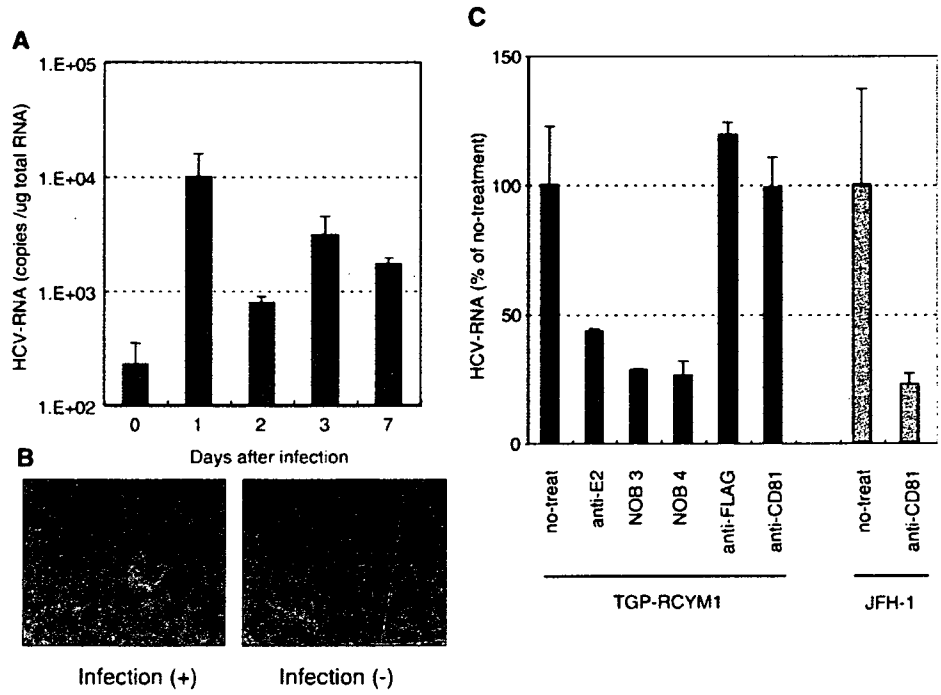

Fig. 6. Infectivity of HCV-LPs secreted from TGP-cultured RCYM1 cells and neutralization of the infection. (A) Kinetics of HCV RNA after the infection of HCV-LPs. Huh-7.5.1 cells were infected with HCV-LPs and harvested at days 0, 1, 2, 3, and 7. HCV RNAs in the cells were determined by real-time RT-PCR. (B) Huh-7.5.1 cells infected with HCV-LPs (upper panel) or without infection (lower panel) were cultured for 4 days, followed by immunostaining with anti-NS5A antibody. Nuclei were counterstained with 4′,6-diamidino-2-phenylindole (DAPI). (C) Huh-7.5.1 cells were infected with HCV-LPs after pretreatment with anti-E2 antibody AP33, neutralization of binding (NOB) antibodies, or anti-FLAG antibody. Anti-human CD81 antibody was preincubated with Huh-7.5.1 cells prior to the infection. Huh-7.5.1 cells were infected with HCV-LPs derived from TGP-cultured RCYM1cells or JFH1 virus and incubated for 4 days; HCV RNAs in the cells were determined by real-time RT-PCR. The inhibition rate is given as the percentage of the no-treatment controls. Average values with standard deviations in triplicate samples are shown. Closed bars, HCV-LPs secreted from TGP-cultured RCYM1 cells; shaded bars, JFH1 virus.

and 26% in the presence of AP33, NOB3, and NOB4, respectively. No reduction of viral RNA in infected cells was observed following treatment with anti-FLAG antibody. Thus, the present results suggest that viral envelope proteins play a crucial role in the infectivity of HCV-LPs produced by RCYM1 cells cultured in TGP. We further tested anti-CD81 antibody for inhibition of the virus infection in our system. As shown in Fig. 6C, pretreatment of the cells with the anti-CD81 antibody resulted in no inhibition of the intracellular HCV RNA level in the infected cells. In contrast, under the same condition of treatment, the antibody efficiently inhibited the infection of JFH-1 virus, which was produced from the HCV JFH-1 molecular clone as previously described (Wakita et al., 2005; Zhong et al., 2005), suggesting that CD81 has no or little, if any, need for the infection of HCV produced in our system.

Potential use of the TGP culture system for HCV production and evaluation of antiviral agents

In a recent report, Lindenbach et al. (2005) found that a cell culture system supporting complete replication of an HCV genotype 2a clone is useful for the evaluation of antiviral drugs. However, to date this complete HCV culture system has not been extended to genotype 1b, which is more frequently detected in patients with hepatitis C and is the most difficult to treat.

We show here the potential utility of the TGP culture of RCYM1 cells for evaluating anti-HCV drugs (Fig. 7). Intracellular HCV RNA levels in TGP-cultured RCYM1 cell spheroids were reduced by 90% after 3 days of culture with 100 IU/ml of IFN-α (Fig. 7A). Likewise, the extracellular HCV particle level, which was calculated using the HCV RNA copy number of the 1.18 g/ml supernatant fraction, was reduced by 89% by IFN-α treatment (Fig. 7B). Moreover, the production of HCV particles was inhibited by treatment with 100 μM RBV to the same degree (85%) as intracellular HCV RNA (Fig. 7B). The level of HCV RNA detected in the 1.04 g/ml fraction of the culture supernatant of the untreated group was approximately one fourteenth of that in the 1.18 g/ml fraction, and the level increased with the addition of IFN-α or RBV (Fig. 7B). Although the mechanism underlying this increase is unknown, a similar phenomenon was observed when several highly cytotoxic agents were evaluated using TGP-RCYM1 cultures (data not shown). It is therefore likely that some cellular proteins associated with HCV RNA are released into the culture supernatant as a result of cell death caused by the moderate cytotoxic effects of IFN and RBV.

Collectively, these results demonstrate that the HCV production model based on TGP culture is useful for evaluating HCV particle production and the inhibitory effects of anti-HCV drugs.

Discussion

In the present report, we describe that HCV-LPs are assembled and released from Huh-7 cells harboring a dicistronic genome-length Con1 HCV RNA in two independent 3D culture systems. The HCV-LPs closely resemble virus-like particles detected in the sera of patients with hepatitis C in terms of both particle size and morphology. The HCV-LPs released into the culture supernatant have a buoyant density of approximately 1.18 g/ml, which is much higher than that of putative HCV particles isolated from patient sera reported previously (Andre et al., 2002; Kanto et al., 1994; Nakajima et al., 1996; Trestard et al., 1998) and slightly higher than the average density of virus particles produced with the JFH-1 isolate (Wakita et al., 2005). One possible explanation is that the HCV particles are highly bound to lipids and low-density lipoproteins in patient sera. In agreement with a recent report (Wakita et al., 2005), our EM examination demonstrated that HCV-LPs are 50–60 nm in diameter and are composed of core-like particles with a diameter of approximately 30 nm that are surrounded by ER-derived E1/

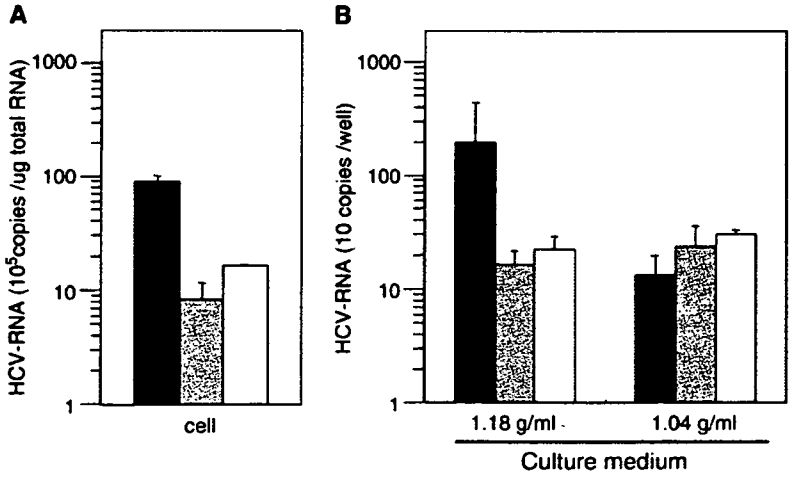

Fig. 7. Inhibition of HCV-LP production by IFN and RBV. TGP-cultured RCYM1 cells were treated with 100 IU/ml IFN-α or 100 μM RBV, and HCV RNAs in the cells (A) and in the culture media (B) were then determined. Culture media from each sample were fractionated by sucrose gradient centrifugation and HCV-LP positive (1.18 g/ml) and negative (1.04 g/ml) fractions were assayed. Average values with standard deviations in triplicate samples are shown. Closed bars, no-treatment control; shaded bars, IFN-α; open bars, RBV.

E2 proteins. These particles are observed at the ER membranes and in dilated cisternae of the ER, suggesting that the interaction of the ER membrane containing HCV envelope proteins with the viral core protein drives the budding process of HCV particles into the ER lumen.

Although studies on the ultrastructure and morphogenesis of HCV-LPs have been conducted using recombinant viral vectors carrying HCV structural protein genes (Baumert et al., 1998; Blanchard et al., 2002, 2003), the present study provides the first visual evidence of assembly and budding of HCV particles in a heterologous expression system in which a full-length viral genome is replicating and the viral particles are secreted into the culture medium. We also demonstrated that the HCV-LPs produced in our 3D culture system are infectious and that their infection is prevented by the monoclonal antibody AP33 directed against E2 (Owsianka et al., 2005) as well as by NOB antibodies (Ishii et al., 1998), which are sera of patients naturally resolving from chronic hepatitis C and exhibiting neutralizing activity. This result is consistent with the recent demonstration that E2 is required for the infectivity of JFH-1 virus (Wakita et al., 2005). It has been shown that CD81 interacts with E2 (Pileri et al., 1998) and that anti-CD81 antibodies or a soluble CD81 fragment block the infection of Huh-7 cells with either pseudotyped retroviral particles, JFH-1 virus or J6/JFH1 chimera (Lindenbach et al., 2005; Netski et al., 2005; Wakita et al., 2005; Zhong et al., 2005). Inconsistent with these studies, however, we found that anti-CD81 antibody did not inhibit the virus infection in our system. Although CD81 is considered to represent an important component in HCV entry, there are several other candidate cellular receptors for HCV (Bartosch and Cosset, 2006) and a study has demonstrated that in vitro binding of HCV to hepatoma cell lines was not inhibited by the anti-CD81 antibody (Sasaki et al., 2003).

In a previous report (Aizaki et al., 2003), we describe the production and release of infectious HCV particles from a human hepatocellular carcinoma-derived cell line, FLC4, using RFB culture in two experiments: inoculation of cells with infectious plasma from an HCV carrier and transfection of cells with viral RNA transcribed from the full-length cDNA of genotype 1a, which is known to infect chimpanzees. These findings prompted us to use the RFB system to create a culture model of HCV production based on genome-length dicistronic viral RNA, which has not been found to produce viral particles in standard monolayer cultures. As expected, HCV-LPs were produced and secreted into the medium during RFB culture of RCYM1 cells, whereas virus production was not observed in the conventional monolayer culture of RCYM1 cells. The presence of the viral envelope protein(s) on the HCV-LPs obtained in the RFB culture was strongly suggested from their density analysis with and without NP40 treatment.

We also created another 3D environment supportive of RCYM1 culture using TGP, a chemically synthesized biocompatible polymer which has a sol-gel transition temperature, thus enabling us to culture cells three-dimensionally in the gel phase at 37 °C and to harvest them in the sol phase at 4 °C, without enzyme digestion (Yoshioka et al., 1994). In contrast to other matrix gels made from conventional natural polymers and developed for 3D culture, including matrigel (Kleinman et al., 1986), collagen gel (Lawler et al., 1983), and soft agar, TGP has several advantages that allow us to investigate the functional characteristics of epithelial cells, their tissue-like morphology, and their potential clinical applications. The use of 3D culture materials other than TGP requires treatment with appropriate digestive enzymes or heating to collect cells grown as spheroids from the culture media, and the matrices may damage the cultured cells to some extent. Thus, it is difficult to keep the viable cells in a functionally and structurally intact. In addition, because matrigel and collagen gel are made from animal or tumor tissue, the possibility that certain pathogens or unidentified factors might influence cell function cannot be excluded. In the present study, we found that Huh-7 and RCYM1 cells formed an organized structure of spheroids after 7–10 days of culture in TGP, and that HCV-LPs were assembled and released from RCYM1 spheroids, as observed in RFB culture. It can be ruled out that HCV-LPs, RNA, and core protein detected in the TGP culture supernatant are released by damaged and/or broken cells because neither digestive enzymes nor heating is used in the culture procedures and no cell damage has been observed in the cultures.

It remains to be clarified why HCV particles were produced from Huh-7 cells harboring the genome-length dicistronic HCV RNA more efficiently in the 3D cultures than in the monolayer cultures. However, this might be related to the fact that directional protein transport in hepatocytes occurs more readily in 3D culture. EM examination demonstrated that, in the RFB and TGP culture systems, human hepatoma cells, such as Huh-7, FLC4, and FLC5 cells, self-assemble into spheroids with possible polarized morphology in which microvilli develop on the cell surface and channels resembling bile canaliculi and junction structures are created in the intercellular spaces (Aizaki et al., 2003; Iwahori et al., 2003). In contrast, human hepatoma cells adhere when grown on a plastic surface, growing as a flat monolayer without exhibiting the characteristics of polarized epithelium. In general, the interaction of viruses with polarized epithelia in the host is one of the key steps in the viral life cycle. A variety of viruses, especially enveloped viruses, mature and bud from distinct membrane domains of the host cells (Compans, 1995; Garoff et al., 1998; Schmitt and Lamb, 2004; Takimoto and Portner, 2004). For example, several respiratory viruses, such as influenza virus, parainfluenza virus, rhinovirus, and respiratory syncytial virus, are released preferentially from the apical surface. Conversely, other viruses egress from the basolateral membrane; these include vesicular stomatitis virus, Semliki Forest virus, vaccinia virus, and certain retroviruses. Thus, it is likely that more organized intracellular trafficking pathways exist in the 3D culture of Huh-7-derived cells, thereby driving the assembly and release of HCV.

The efficient production of HCV in 3D cultures could also be due to the reduction of HCV RNA replication and/or translation in 3D cultures as compared to those in monolayer cultures. RNA replication and/or translation of HCV replicons in Huh-7 cells are highly dependent on host cell growth (Pietschmann et al., 2001). In the present study, we found that the slow growth of spheroids resulted in reduced expression of HCV protein and

viral RNA in 3D-cultured RCYM1 cells compared to that in monolayer cultures containing similar cell numbers. The doubling time of cells grown in TGP or RFB culture was approximately twice that observed in monolayer culture. Although it is possible that amino acid substitutions of culture-adaptive mutations contribute to interference with virus production, another possibility might be that in cases of certain HCV clones, higher expression of the viral proteins leads to their misfolding, thereby precluding the formation of virus particles.

Complete cell culture systems for HCV have recently been developed (Lindenbach et al., 2005; Wakita et al., 2005; Zhong et al., 2005) using a genotype 2a isolate, JFH-1, obtained from a Japanese patient with fulminant hepatitis (Date et al., 2004; Kato et al., 2001, 2003). Unlike many other HCV isolates, JFH-1-based subgenomic replicons do not require culture-adaptive mutations for efficient RNA replication (Kato et al., 2003). Transfection of Huh-7 cells with the full-length JFH-1 genome or a chimeric genome using JFH-1 and J6 results in the efficient production of infectious HCV (Lindenbach et al., 2005; Wakita et al., 2005; Zhong et al., 2005). This newly established HCV culture system is undoubtedly useful for a variety of HCV studies; however, these systems rely on the JFH-1 replicase (NS3 to 5B) and little is known about the reasons that this particular isolate permits efficient HCV production. Virus yield in the 3D systems presented here is significantly lower than that in systems based on JFH-1; it seems that 0.1–1 copies of HCV RNA/cell/day are generated and assembled into viral particles. The ratio of viral RNA to the core protein in these fractions is approximately 10^5 RNA copies/1 fmol of the core. Although only moderate production of HCV particles is observed in 3D culture of RCYM1 cells, this is the first study to demonstrate the production of infectious HCV particles derived from genotype 1b, which is highly prevalent worldwide and is thought to present a higher risk of developing hepatocellular carcinoma and/or cirrhosis than infections with other HCV types (Bruno et al., 1997; Silini et al., 1996). The findings of the present study may also suggest that an extremely high efficiency of viral replication, such as that observed in the case of JFH-1 isolate, is not needed to produce HCV particles in 3D cultures of Huh-7 cells. Heller et al. (2005) report HCV virion production in a culture transfected with the genomic cDNA of genotype 1b; however, the infectivity of the virus particles remains to be determined. More recently, it was shown that chimeric HCV containing structural proteins of genotypes 1a, 1b, or 3a was produced from fusion of the core to the p7 or NS2 region with downstream nonstructural regions of JFH1 clone, but that intergenotypic chimeras frequently yielded lower titers of infectious HCV compared to JFH1 or J6/JFH1 chimera (Pietschmann et al., personal communication). The 3D culture system described in the present study might be a helpful method of increasing the efficiency of assembly and release of intergenotypic chimeric HCV.

In summary, we found that the expression of dicistronic genome-length Con1 HCV RNA of genotype 1b in 3D-cultured Huh-7 cells yields infectious virus particles, and we demonstrated the usefulness for producing HCV particles of two 3D culture systems based on RFB and TGP, in which human hepatoma cells can assemble into spheroids with potentially polarized morphology. HCV morphogenesis occurs in a complex cellular environment in which host factors may either enhance or reduce the assembly and budding process. The culture system described here will allow us to further study viral morphogenesis and the biophysical properties of HCV particles, and it provides a new tool for the future development of anti-HCV drugs.

Materials and methods

Cell lines bearing dicistronic HCV RNAs

To generate a stable cell line harboring genome-length dicistronic HCV RNA, we electroporated 10^7 Huh-7 cells with 50 μg of the RNA transcribed from a plasmid pFKI389neo/core-3′/NK5.1 (Pietschmann et al., 2002). The cells were maintained in Dulbecco's modified Eagle's medium with 10% fetal bovine serum and 0.5 mg/ml G418 (Promega). After stringent selection for 3 weeks, a fast-growing clone was isolated and designated as RCYM1. A Huh-7-derived cell line, 5–15, harboring a subgenomic replicon (Lohmann et al., 1999) was also used.

3D cell cultures

The RFB system (Able, Japan) was manipulated as described previously (Aizaki et al., 2003) with minor modifications. Briefly, the RFB column, being filled with 4 ml of porous carrier beads made from polyvinyl alcohol, seeded with 1×10^7 of RCYM1 or 5–15 cells. The cells were cultured in ASF104 medium (Ajinomoto, Japan) supplemented with 4 g/l of D-glucose, 2% fetal calf serum, and 0.5 mg/ml of G418 (Promega). TGP (Mebiol Gel MB-10; Mebiol, Japan) was supplied as a lyophilized form and its aqueous solution was prepared before use as previously described (Hishikawa et al., 2004; Nagaya et al., 2004; Yoshioka et al., 1994). Briefly, TGP in a flask was dissolved in 10 ml of the culture medium and was maintained at 4 °C overnight. To prepare HCV particles, we suspended 5×10^6 cells of RCYM1 in 10 ml of TGP solution and aliquots were poured into a multi-well plate. Upon warming to 37 °C, the TGP solution quickly turned into a gel form, and 3 volumes of the culture medium were added to cover the gel. To recover spheroid cells and the culture supernatant after cultivation, we subjected the cultured plate to a temperature of 4 °C for 10 min to dissolve the gel. In order to separate spheroid cells from the culture medium, we subsequently centrifuged the TGP culture diluted with the overlaid culture medium at 1000×*g* for 5 min.

Sucrose density gradient centrifugation

The culture medium collected from the RFB or TGP was centrifuged at 8000 × *g* for 50 min to remove all cellular debris, after which the supernatant was centrifuged at 25,000 rpm at 4 °C for 4 h with an SW28 rotor (Beckman). The precipitant was suspended in 1 ml of TNE buffer [10 mM Tris–HCl (pH 7.8), 1 mM EDTA, 100 mM NaCl] and was then layered on top of continuous 10–60% (wt/vol) sucrose gradient in TNE buffer,

followed by centrifugation at 35,000 rpm at 4 °C for 14 h with an SW41E rotor (Beckman). Fractions (1 ml each) were collected from the top of the tube (12 fractions in total). The density of each fraction was determined by the weight of 100 μl of the fraction. For NP40 treatment, 0.5 ml of the TNE-suspended sample as described above was supplemented with 10 μl of RNase inhibitor (Takara, Japan) and 5 μl of 1M DTT, which was diluted by adding NP40 solution to a final concentration of 0.2%. After incubation at 4 °C for 20 min, the sample was fractionated by discontinuous 10–60% sucrose gradient centrifugation.

Quantitation of HCV RNA and core protein

Total RNA was extracted from cells and from the culture medium using TRIZOL (Invitrogen) and a QIAamp Viral RNA Mini spin column (Qiagen), respectively. Real-time RT-PCR was performed using TaqMan EZ RT-PCR Core Reagents (PE Applied Biosystems), as described previously (Aizaki et al., 2004; Suzuki et al., 2005). HCV core antigen within cells and culture medium was measured by immunoassay (Ortho HCV-Core ELISA Kit; Ortho-Clinical Diagnotics), following the manufacturer's instructions.

Western blot analysis

The protein concentration of cells recovered from monolayer or 3D cultures was determined by BCA Protein Assay Kit (Pierce). Aliquots of samples were analyzed by sodium dodecyl sulfate–polyacrylamide gel electrophoresis (SDS–PAGE) and transferred to polyvinylidene difluoride membranes (Immobilon; Millipore, Japan) using a semidry blotter. After overnight incubation at 4 °C in blocking buffer (Dainippon Pharmaceuticals, Japan) with 0.2% Tween 20, the membranes were incubated with appropriately diluted anti-HCV core (Anogen) and anti-NS5A (Austral Biologicals) monoclonal antibody, followed by incubation with horseradish peroxidase conjugated anti-mouse immunoglobulin G (Cell Signaling). The blots were then washed and developed with enhanced SuperSignal West Pico Chemiluminecent Substrate (Pierce).

Immunocytochemistry

For NS5A staining, infected cells cultured on collagen-coated coverslips were washed with phosphate buffered saline (PBS) and fixed with 4% paraformaldehyde at 4 °C for 30 min, followed by permeabilization with PBS containing 0.2% TritonX-100. After preincubation with BlockAce (Dainippon Pharmaceuticals), the samples were stained using mouse anti-NS5A antibody and rhodamine-conjugated goat anti-mouse IgG (ICN Pharmaceuticals) as the first and second antibodies, respectively.

Electron microscopy

To visualize HCV-LPs secreted into the medium, we concentrated and adsorbed sucrose density fractions prepared as described above onto carbon-coated grids for 1 min. The grids were stained with 1% uranyl acetate for 1 min and examined under a Hitachi H-7600 transmission electron microscope. To prepare thin sections of HCV-LPs, we prefixed precipitated HCV-LPs in 2% glutaraldehyde–0.1 M cacodylate buffer at 4 °C overnight, followed by three rounds of washing with 0.1 M cacodylate buffer. The samples were then postfixed in 2% osmium tetroxide at 4 °C for 2 h, dehydrated in a graded series of ethanol solutions followed by propylene oxide, and embedded in a mixture of EPON 812, dodecenyl succinic anhydride (DDSA), methyl nadic anhydrate (MNA), and 2,4,6-tri (dimethylaminomethyl) phenol (DMP-30) at 60 °C for 2 days. Thin sections (80 nm) were stained with uranyl acetate and lead citrate. For electron microscopy of RCYM1 cells cultured in TGP, the cells were prefixed in 2% glutaraldehyde–0.1 M cacodylate buffer at 4 °C for 1 h and washed three times with 0.1 M cacodylate buffer, followed by postfixation in 2% osmium tetroxide for 3 h. After dehydration in a graded series of ethanol solutions and propylene oxide, the cells were embedded in a mixture of Epoxy 812, DDSA, MNA, and DMP-30 at 60 °C for 2 days. Thin sections (60–80 nm) were stained with 2% uranyl acetate.

Immunoelectron microscopy

HCV-LP samples were adsorbed on formvar-carbon grids and then floated for 30 min on a drop of BlockAce. Diluted anti-E2 mouse antibody was then applied for 1 h. After three rounds of washing, diluted anti-mouse IgG conjugated with 5-nm gold particles was applied for 1 h, and the grids were then stained with 1% uranyl acetate. In order to perform immunoelectron microscopy of TGP cultures using silver-intensified immunogold labeling, we fixed the cells in 4% paraformaldehyde–0.1% glutaraldehyde with 0.15 M HEPES buffer at 4 °C, followed by incubation with either anti-core rabbit antibody or anti-E1 mouse antibody overnight. After several washings, anti-rabbit or anti-mouse secondary antibody coupled with 1.4-nm-diameter gold particles (Nanoprobes) was applied overnight. The samples were then washed and fixed in 2% glutaraldehyde in 0.1 M sodium cacodylate buffer (pH 7.4) for 3 h, followed by enlargement of the gold particles with an HQ-Silver Enhancement Kit (Nanoprobes). For double staining with anti-E1 and anti-core antibodies, the cells were fixed in 7% paraformaldehyde–0.25 M sucrose in 0.03% picric acid–0.05 M cacodylate buffer at pH 7.4. Ten-nanometer gold particle-coupled anti-rabbit and 5-nm gold particle-coupled anti-mouse antibodies were used as secondary antibodies.

Assays for the infectivity of HCV-LPs and neutralization of the infection

Cell supernatant from 3D-cultured RCYM1 cells was centrifuged at 8000 × *g* for 50 min to remove all cellular debris, after which the supernatant was centrifuged at 25,000 rpm at 4 °C for 4 h with an SW28 rotor. The precipitant was suspended in 0.2–0.5 ml of ASF104 medium and the aliquot containing approximately 1×10^5 HCV RNA copies was used as each inoculum. Huh-7.5.1

cells (provided by Dr. F. V. Chisari, The Scripps Research Institute) (Zhong et al., 2005), which were seeded at a density of 10^4 cells/well in a 48-well plate 24 h before infection. The inocula were incubated for 3 h, followed by 3 rounds of washing with PBS and the addition of complete medium. For the kinetics assay, cells were harvested 0, 1, 2, 3, and 7 days after infection and the amount of intracellular HCV RNA was quantified as described above. Infection with HCV-LP was determined after 4 days by immunofluorescence staining for HCV NS5A. In the neutralization assay, the HCV-LP samples were incubated with the anti-E2 antibody AP33 (Owsianka et al., 2005) at 10 μg/ml (kindly provided by Dr. A. H. Patel, University of Glasgow, UK), with the human sera with high titers of NOB antibodies NOB3 and NOB4 (Ishii et al., 1998), or with anti-FLAG antibody (Sigma) at 10 μg/ml for 1 h at 37 °C prior to infection. Anti-human CD81 antibody (BD Pharmigen) at 10 μg/ml was preincubated with Huh-7.5.1 cells for 1 h at 37 °C, followed by being washed with PBS three times. HCV-LP derived from TGP-cultured RCYM1 cells or JFH1 virus was incubated with these cells, as mentioned above. JFH1 virus was prepared from pJFH1 (Wakita et al., 2005), which contains the full-length cDNA of JFH1 isolate and was kindly provided by T. Wakita (Tokyo Metropolitan Institute for Neuroscience, Japan), as described (Wakita et al., 2005). The cells were harvested 4 days after infection and neutralizing activity was assessed by quantifying the amount of intracellular HCV RNA as described above.

Assay for anti-HCV-LP production

At the initiation of the 3D culture of RCYM1 cells (5×10^5 in 1 ml TGP), 100 IU/ml IFN-α (Sumiferon 300; Sumitomo Pharmaceuticals, Japan), or 100 μM RBV (MP Biomedicals, Germany) were added and the cells were cultured for 5 days. Culture media were harvested and fractionated by sucrose density centrifugation as described above. Total RNAs were extracted from aliquots of 1.18 g/ml (HCV-LP positive) and 1.04 g/ml (HCV-LP-negative) fractions, followed by quantification of viral RNA.

Acknowledgments

The authors would like to thank Francis V. Chisari of The Scripps Research Institute, Arvind H. Patel of the University of Glasgow, and Takaji Wakita of Tokyo Metropolitan Institute for Neuroscience for providing Huh-7.5.1 cells, anti-E2 antibody, and pJFH1, respectively. We also thank Mami Matsuda, Tetsu Shimoji, and Makiko Yahata for technical assistance, and Tomoko Mizoguchi for her secretarial work. This work was supported in part by a grant for Research on Health Sciences focusing on Drug Innovation from the Japan Health Sciences Foundation; by grants-in-aid from the Ministry of Health, Labor and Welfare; by a Sasagawa Scientific Research Grant from the Japan Science Society; and by the program for Promotion of Fundamental Studies in Health Sciences of the National Institute of Biomedical Innovation (NBIO), Japan; and by the New Energy and Industrial Technology Development Organization (NEDO) of Japan.

References

Aizaki, H., Nagamori, S., Matsuda, M., Kawakami, H., Hashimoto, O., Ishiko, H., Kawada, M., Matsuura, T., Hasumura, S., Matsuura, Y., Suzuki, T., Miyamura, T., 2003. Production and release of infectious hepatitis C virus from human liver cell cultures in the three-dimensional radial-flow bioreactor. Virology 314, 16–25.

Aizaki, H., Lee, K.J., Sung, V.M., Ishiko, H., Lai, M.M., 2004. Characterization of the hepatitis C virus RNA replication complex associated with lipid rafts. Virology 324, 450–461.

Andre, P., Komurian-Pradel, F., Deforges, S., Perret, M., Berland, J.L., Sodoyer, M., Pol, S., Brechot, C., Paranhos-Baccala, G., Lotteau, V., 2002. Characterization of low- and very-low-density hepatitis C virus RNA-containing particles. J. Virol. 76, 6919–6928.

Bartosch, B., Cosset, F.L., 2006. Cell entry of hepatitis C virus. Virology (Electronic publication ahead of print).

Baumert, T.F., Ito, S., Wong, D.T., Liang, T.J., 1998. Hepatitis C virus structural proteins assemble into viruslike particles in insect cells. J. Virol. 72, 3827–3836.

Blanchard, E., Brand, D., Trassard, S., Goudeau, A., Roingeard, P., 2002. Hepatitis C virus-like particle morphogenesis. J. Virol. 76, 4073–4079.

Blanchard, E., Hourioux, C., Brand, D., Ait-Goughoulte, M., Moreau, A., Trassard, S., Sizaret, P.Y., Dubois, F., Roingeard, P., 2003. Hepatitis C virus-like particle budding: role of the core protein and importance of its Asp111. J. Virol. 77, 10131–10138.

Blight, K.J., Kolykhalov, A.A., Rice, C.M., 2000. Efficient initiation of HCV RNA replication in cell culture. Science 290, 1972–1974.

Blight, K.J., McKeating, J.A., Rice, C.M., 2002. Highly permissive cell lines for subgenomic and genomic hepatitis C virus RNA replication. J. Virol. 76, 13001–13014.

Bruno, S., Silini, E., Crosignani, A., Borzio, F., Leandro, G., Bono, F., Asti, M., Rossi, S., Larghi, A., Cerino, A., Podda, M., Mondelli, M.U., 1997. Hepatitis C virus genotypes and risk of hepatocellular carcinoma in cirrhosis: a prospective study. Hepatology 25, 754–758.

Choo, Q.L., Kuo, G., Weiner, A.J., Overby, L.R., Bradley, D.W., Houghton, M., 1989. Isolation of a cDNA clone derived from a blood-borne non-A, non-B viral hepatitis genome. Science 244, 359–362.

Choo, Q.L., Richman, K.H., Han, J.H., Berger, K., Lee, C., Dong, C., Gallegos, C., Coit, D., Medina-Selby, R., Barr, P.J., et al., 1991. Genetic organization and diversity of the hepatitis C virus. Proc. Natl. Acad. Sci. U.S.A. 88, 2451–2455.

Compans, R.W., 1995. Virus entry and release in polarized epithelial cells. Curr. Top. Microbiol. Immunol. 202, 209–219.

Date, T., Kato, T., Miyamoto, M., Zhao, Z., Yasui, K., Mizokami, M., Wakita, T., 2004. Genotype 2a hepatitis C virus subgenomic replicon can replicate in HepG2 and IMY-N9 cells. J. Biol. Chem. 279, 22371–22376.

Davis, G.L., Wong, J.B., McHutchison, J.G., Manns, M.P., Harvey, J., Albrecht, J., 2003. Early virologic response to treatment with peginterferon alfa-2b plus ribavirin in patients with chronic hepatitis C. Hepatology 38, 645–652.

Frese, M., Pietschmann, T., Moradpour, D., Haller, O., Bartenschlager, R., 2001. Interferon-alpha inhibits hepatitis C virus subgenomic RNA replication by an MxA-independent pathway. J. Gen. Virol. 82, 723–733.

Garoff, H., Hewson, R., Opstelten, D.J., 1998. Virus maturation by budding. Microbiol. Mol. Biol. Rev. 62, 1171–1190.

Grakoui, A., McCourt, D.W., Wychowski, C., Feinstone, S.M., Rice, C.M., 1993. Characterization of the hepatitis C virus-encoded serine proteinase: determination of proteinase-dependent polyprotein cleavage sites. J. Virol. 67, 2832–2843.

Guo, J.T., Bichko, V.V., Seeger, C., 2001. Effect of alpha interferon on the hepatitis C virus replicon. J. Virol. 75, 8516–8523.

Heller, T., Saito, S., Auerbach, J., Williams, T., Moreen, T.R., Jazwinski, A., Cruz, B., Jeurkar, N., Sapp, R., Luo, G., Liang, T.J., 2005. An in vitro model of hepatitis C virion production. Proc. Natl. Acad. Sci. U.S.A. 102, 2579–2583.

Hijikata, M., Kato, N., Ootsuyama, Y., Nakagawa, M., Shimotohno, K., 1991. Gene mapping of the putative structural region of the hepatitis C virus genome by in vitro processing analysis. Proc. Natl. Acad. Sci. U.S.A. 88, 5547–5551.

Hishikawa, K., Miura, S., Marumo, T., Yoshioka, H., Mori, Y., Takato, T., Fujita, T., 2004. Gene expression profile of human mesenchymal stem cells during osteogenesis in three-dimensional thermoreversible gelation polymer. Biochem. Biophys. Res. Commun. 317, 1103–1107.

Ikeda, M., Yi, M., Li, K., Lemon, S.M., 2002. Selectable subgenomic and genome-length dicistronic RNAs derived from an infectious molecular clone of the HCV-N strain of hepatitis C virus replicate efficiently in cultured Huh7 cells. J. Virol. 76, 2997–3006.

Ishii, K., Rosa, D., Watanabe, Y., Katayama, T., Harada, H., Wyatt, C., Kiyosawa, K., Aizaki, H., Matsuura, Y., Houghton, M., Abrignani, S., Miyamura, T., 1998. High titers of antibodies inhibiting the binding of envelope to human cells correlate with natural resolution of chronic hepatitis C. Hepatology 28, 1117–1120.

Iwahori, T., Matsuura, T., Maehashi, H., Sugo, K., Saito, M., Hosokawa, M., Chiba, K., Masaki, T., Aizaki, H., Ohkawa, K., Suzuki, T., 2003. CYP3A4 inducible model for in vitro analysis of human drug metabolism using a bioartificial liver. Hepatology 37, 665–673.

Kanto, T., Hayashi, N., Takehara, T., Hagiwara, H., Mita, E., Naito, M., Kasahara, A., Fusamoto, H., Kamada, T., 1994. Buoyant density of hepatitis C virus recovered from infected hosts: two different features in sucrose equilibrium density-gradient centrifugation related to degree of liver inflammation. Hepatology 19, 296–302.

Kato, T., Furusaka, A., Miyamoto, M., Date, T., Yasui, K., Hiramoto, J., Nagayama, K., Tanaka, T., Wakita, T., 2001. Sequence analysis of hepatitis C virus isolated from a fulminant hepatitis patient. J. Med. Virol. 64, 334–339.

Kato, T., Date, T., Miyamoto, M., Furusaka, A., Tokushige, K., Mizokami, M., Wakita, T., 2003. Efficient replication of the genotype 2a hepatitis C virus subgenomic replicon. Gastroenterology 125, 1808–1817.

Kawada, M., Nagamori, S., Aizaki, H., Fukaya, K., Niiya, M., Matsuura, T., Sujino, H., Hasumura, S., Yashida, H., Mizutani, S., Ikenaga, H., 1998. Massive culture of human liver cancer cells in a newly developed radial flow bioreactor system: ultrafine structure of functionally enhanced hepatocarcinoma cell lines. In Vitro Cell. Dev. Biol. Anim. 34, 109–115.

Kleinman, H.K., McGarvey, M.L., Hassell, J.R., Star, V.L., Cannon, F.B., Laurie, G.W., Martin, G.R., 1986. Basement membrane complexes with biological activity. Biochemistry 25, 312–318.

Lawler, E.M., Miller, F.R., Heppner, G.H., 1983. Significance of three-dimensional growth patterns of mammary tissues in collagen gels. In Vitro 19, 600–610.

Lindenbach, B.D., Evans, M.J., Syder, A.J., Wolk, B., Tellinghuisen, T.L., Liu, C.C., Maruyama, T., Hynes, R.O., Burton, D.R., McKeating, J.A., Rice, C.M., 2005. Complete replication of hepatitis C virus in cell culture. Science 309, 623–626.

Lohmann, V., Korner, F., Koch, J., Herian, U., Theilmann, L., Bartenschlager, R., 1999. Replication of subgenomic hepatitis C virus RNAs in a hepatoma cell line. Science 285, 110–113.

Manns, M.P., McHutchison, J.G., Gordon, S.C., Rustgi, V.K., Shiffman, M., Reindollar, R., Goodman, Z.D., Koury, K., Ling, M., Albrecht, J.K., 2001. Peginterferon alfa-2b plus ribavirin compared with interferon alfa-2b plus ribavirin for initial treatment of chronic hepatitis C: a randomised trial. Lancet 358, 958–965.

Matsuura, T., Kawada, M., Hasumura, S., Nagamori, S., Obata, T., Yamaguchi, M., Hataba, Y., Tanaka, H., Shimizu, H., Unemura, Y., Nonaka, K., Iwaki, T., Kojima, S., Aizaki, H., Mizutani, S., Ikenaga, H., 1998. High density culture of immortalized liver endothelial cells in the radial-flow bioreactor in the development of an artificial liver. Int. J. Artif. Organs 21, 229–234.

Nagaya, M., Kubota, S., Suzuki, N., Tadokoro, M., Akashi, K., 2004. Evaluation of thermoreversible gelation polymer for regeneration of focal liver injury. Eur. Surg. Res. 36, 95–103.

Nakajima, N., Hijikata, M., Yoshikura, H., Shimizu, Y.K., 1996. Characterization of long-term cultures of hepatitis C virus. J. Virol. 70, 3325–3329.

Netski, D.M., Mosbruger, T., Depla, E., Maertens, G., Ray, S.C., Hamilton, R.G., Roundtree, S., Thomas, D.L., McKeating, J., Cox, A., 2005. Humoral immune response in acute hepatitis C virus infection. Clin. Infect. Dis. 41, 667–675.

Owsianka, A., Tarr, A.W., Juttla, V.S., Lavillette, D., Bartosch, B., Cosset, F.L., Ball, J.K., Patel, A.H., 2005. Monoclonal antibody AP33 defines a broadly neutralizing epitope on the hepatitis C virus E2 envelope glycoprotein. J. Virol. 79, 11095–11104.

Pietschmann, T., Lohmann, V., Rutter, G., Kurpanek, K., Bartenschlager, R., 2001. Characterization of cell lines carrying self-replicating hepatitis C virus RNAs. J. Virol. 75, 1252–1264.

Pietschmann, T., Lohmann, V., Kaul, A., Krieger, N., Rinck, G., Rutter, G., Strand, D., Bartenschlager, R., 2002. Persistent and transient replication of full-length hepatitis C virus genomes in cell culture. J. Virol. 76, 4008–4021.

Pileri, P., Uematsu, Y., Campagnoli, S., Galli, G., Falugi, F., Petracca, R., Weiner, A.J., Houghton, M., Rosa, D., Grandi, G., Abrignani, S., 1998. Binding of hepatitis C virus to CD81. Science 282, 938–941.

Rosa, D., Campagnoli, S., Moretto, C., Guenzi, E., Cousens, L., Chin, M., Dong, C., Weiner, A.J., Lau, J.Y., Choo, Q.L., Chien, D., Pileri, P., Houghton, M., Abrignani, S., 1996. A quantitative test to estimate neutralizing antibodies to the hepatitis C virus: cytofluorimetric assessment of envelope glycoprotein 2 binding to target cells. Proc. Natl. Acad. Sci. U.S.A. 93, 1759–1763.

Sasaki, M., Yamauchi, K., Nakanishi, T., Kamogawa, Y., Hayashi, N., 2003. In vitro binding of hepatitis C virus to CD81-positive and -negative human cell lines. J. Gastroenterol. Hepatol. 18, 74–79.

Schmitt, A.P., Lamb, R.A., 2004. Escaping from the cell: assembly and budding of negative-strand RNA viruses. Curr. Top. Microbiol. Immunol. 283, 145–196.

Shimizu, Y.K., Feinstone, S.M., Kohara, M., Purcell, R.H., Yoshikura, H., 1996. Hepatitis C virus: detection of intracellular virus particles by electron microscopy. Hepatology 23, 205–209.

Silini, E., Bottelli, R., Asti, M., Bruno, S., Candusso, M.E., Brambilla, S., Bono, F., Iamoni, G., Tinelli, C., Mondelli, M.U., Ideo, G., 1996. Hepatitis C virus genotypes and risk of hepatocellular carcinoma in cirrhosis: a case–control study. Gastroenterology 111, 199–205.

Suzuki, T., Omata, K., Satoh, T., Miyasaka, T., Arai, C., Maeda, M., Matsuno, T., Miyamura, T., 2005. Quantitative detection of hepatitis C virus (HCV) RNA in saliva and gingival crevicular fluid of HCV-infected patients. J. Clin. Microbiol. 43, 4413–4417.

Takimoto, T., Portner, A., 2004. Molecular mechanism of paramyxovirus budding. Virus Res. 106, 133–145.

Trestard, A., Bacq, Y., Buzelay, L., Dubois, F., Barin, F., Goudeau, A., Roingeard, P., 1998. Ultrastructural and physicochemical characterization of the hepatitis C virus recovered from the serum of an agammaglobulinemic patient. Arch. Virol. 143, 2241–2245.

Wakita, T., Pietschmann, T., Kato, T., Date, T., Miyamoto, M., Zhao, Z., Murthy, K., Habermann, A., Krausslich, H.G., Mizokami, M., Bartenschlager, R., Liang, T.J., 2005. Production of infectious hepatitis C virus in tissue culture from a cloned viral genome. Nat. Med. 11, 791–796.

Yi, M.K., Villanueva, R.A., Thomas, D., Wakita, T., Lemon, S.M., 2006. Production of infectious genotype 1a hepatitis C virus (Hutchinson strain) in cultured human hepatoma cells. Proc. Natl. Acad. Sci. U.S.A. 103, 2310–2315.

Yoshioka, H., Mikami, M., Mori, Y., Tsuchida, E., 1994. A synthetic hydrogel with thermoreversible gelation. J. Macromol. Sci. A31, 113–120.

Zhong, J., Gastaminza, P., Cheng, G., Kapadia, S., Kato, T., Burton, D.R., Wieland, S.F., Uprichard, S.L., Wakita, T., Chisari, F.V., 2005. Robust hepatitis C virus infection in vitro. Proc. Natl. Acad. Sci. U.S.A. 102, 9294–9299.

Transworld Research Network
37/661 (2), Fort P.O., Trivandrum-695 023, Kerala, India

SARS, 2006: 107-117 ISBN: 81-7895-208-4 Editor: Tetsuya Mizutani

8 Vaccines for severe acute respiratory syndrome

Koji Ishii
Department of Virology II, National Institute of Infectious Diseases, 1-23-1 Toyama, Shinjuku-ku, Tokyo 162-8640, Japan

Abstract

The SARS-coronavirus (SARS-CoV), which affected over 8000 individuals worldwide and was responsible for over 700 deaths in the 2002–2003 outbreak, caused acute respiratory distress and was highly lethal when it first emerged in 2002. Although public health measures eventually controlled the spread of SARS, the global impact of the epidemic was severe. Given concerns about future outbreaks and a lack of effective treatments for the virus, global research efforts have focused on the development of vaccines against SARS. Treatment with convalescent plasma has achieved some success, suggesting that induction of passive immunity might be useful to combat SARS. The inactivated SARS-CoV vaccine will likely be the first available vaccine against SARS

Correspondence/Reprint request: Dr. Koji Ishii, Department of Virology II, National Institute of Infectious Diseases, 1-23-1, Toyama, Shinjuku-ku, Tokyo 162-8640, Japan. E-mail: kishii@nih.go.jp

since it is relatively easy to produce. However, there are serious concerns about the safety of this vaccine. The spike protein of SARS-CoV has been identified as the major inducer of neutralizing antibodies, while a receptor-binding domain of the S1 subunit of SARS-CoV S protein contains multiple conformational neutralizing epitopes. This suggests that recombinant proteins containing fragments of the S protein might be used to develop safe and effective SARS vaccines. Viral-vector vaccines and DNA vaccines are also an attractive option for SARS vaccines.

Introduction

A new disease called severe acute respiratory syndrome (SARS) originated in China in late 2002 and spread rapidly throughout a number of countries (1). Clinically, SARS is characterized by high fevers, malaise, rigors, headache, dry cough, and progression to interstitial infiltration of the lungs, with an eventual mortality exceeding 10% in many countries. Laboratory findings include lymphopenia, and chest radiographs commonly exhibit unilateral or bilateral infiltrates (2). Following the WHO alert, a number of probable SARS cases were reported in other regions of China, as well as other Asian countries, including Singapore, Taiwan, Indonesia, Thailand, and the Philippines. International travel facilitated its spread to other continents. Before the initial epidemic ended, 8,098 probable cases of SARS, and 774 associated deaths, were reported to the WHO (www.cdc.gov/mmwr/mguide_sars.html). At the time of the outbreak, a global collaborative network to combat SARS was co-ordinated by the WHO. As a result of this international effort, a novel type of coronavirus (SARS-CoV) was identified as the etiologic agent of SARS (3)(4) in March 2003. The genomic sequence of SARS-CoV was completed and we now know that SARS-CoV has all the characteristic features of a coronavirus, but it is quite different from all previously known coronaviruses (group I~III), representing a new group of coronavirus (group IV) (5)(6). SARS-CoV is thought to be a mutant coronavirus transmitted from a wild animal, which has developed the ability to infect humans (5)(7). The SARS-CoV genome is a single-stranded positive-sense RNA sequence, approximately 30 kb in length, containing five major open reading frames encoding non-structural replicase polyproteins and structural proteins. These include spike (S), envelope (E), membrane (M), and nucleocapsid (N) proteins, which are encoded in much the same order and are of similar size to the structural proteins of other coronaviruses (Fig.1). The S protein is involved in receptor binding, fusion, and entry, and is a major inducer of neutralizing antibodies, while the E protein plays a role in viral assembly, the M protein in virus budding, and the N protein in viral RNA packaging (for review, see reference (7)). In a model of MHV infection, S proteins are known to contain important virus-neutralizing epitopes that elicit neutralizing antibody responses in mice (8). The S protein

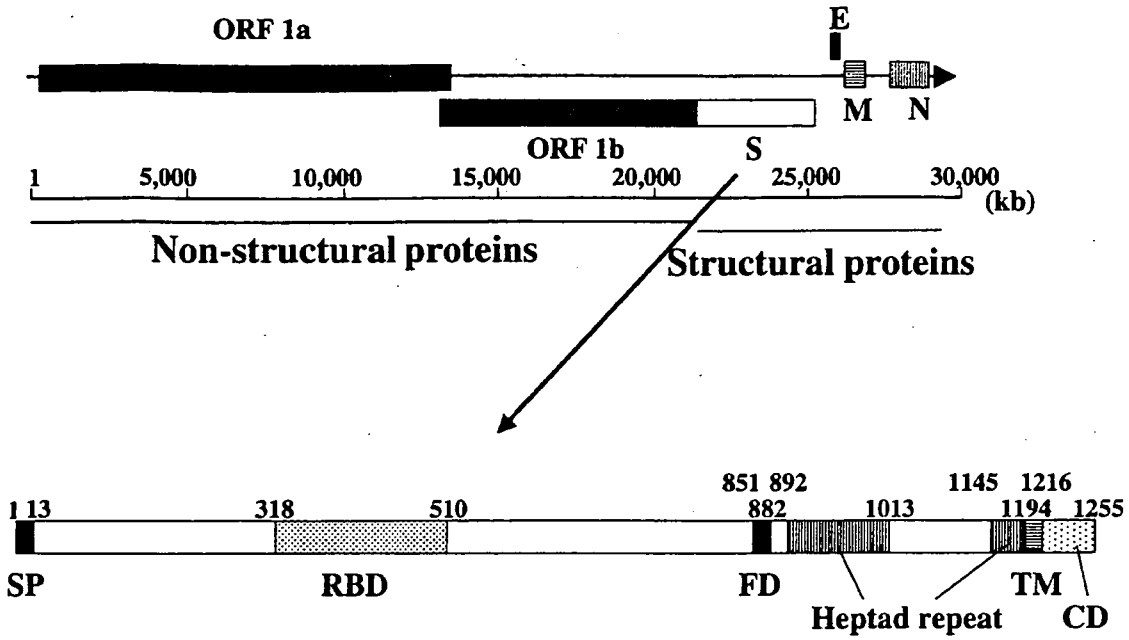

Figure 1. Genome organization and the structure of spike glycoprotein of SARS-CoV. Upper panel: S; spike glycoprotein, E; envelope protein, M, membrane glycoprotein; N, nucleocapsid protein. Lower panel: SP, signal peptide; RBD, receptor binding domain; FD, fusion domain; TM, transmembrane domain; CD, cytoplasm domain. The residue numbers of each region correspond to their amino acid positions in the S protein.

of SARS-CoV consists of a signal peptide and three domains: an extracellular domain, a transmembrane domain, and an intracellular domain. The extracellular domain consists of two subunits: S1 and S2 (7). The S1 subunit is responsible for binding of the virus to its receptor, angiotensin-converting enzyme 2 (ACE2) (9). A fragment located in the middle region of the S1 subunit is the receptor-binding domain (RBD) for ACE2 (10)(11)(12). The S2 subunit, which contains a putative fusion peptide and two heptad repeats (HR1 and HR2), is responsible for fusion between the virus and target cell membranes (Fig.1)(13). This indicates that the S protein may have potential use as a vaccine, resulting in the production of antibodies which prevent virus binding and fusion.

Since the initial outbreak, global research efforts have focused on developing effective vaccines against SARS. This review summarizes the progress made to date with regard to SARS vaccines.

Passive immunization

Treatment with convalescent plasma has been successfully used to treat SARS, suggesting that passive immunity might be a useful approach by which to combat SARS. (14) Subbarao *et al.* (15) have shown that passive transfer of murine neutralizing antibodies can prevent replication of SARS coronavirus in

the respiratory tract. Traggiai *et al.* (16) have isolated human monoclonal antibodies from immortalized B lymphocytes of people recovering from SARS. These antibodies have been shown to neutralize the virus *in vitro*, and to prevent viral replication in a mouse model of SARS-coronavirus infection. Since human serum containing antibodies to SARS-CoV is not available in sufficient amounts, neutralizing antibodies are thought to be a good alterative for passive immunization. Sui *et al.* have investigated the antiviral activity of a human monoclonal antibody to S1 protein that blocks receptor association (17), demonstrating the prophylactic effectiveness of this monoclonal antibody *in vivo* using a mouse model of SARS. (18) Alternatively, in China, pure concentrated human SARS hyperimmunoglobulins for intravenous injection have been prepared from pooled convalescent plasma samples, which are awaiting evaluation. ter Meulen *et al.* (19) have shown that prophylactic administration of a human IgG monoclonal antibody capable of reacting with whole inactivated SARS coronavirus is able to reduce SARS coronavirus replication within the lungs of infected ferrets, as well as prevent the development of SARS-coronavirus-induced macroscopic lung pathology and prevent viral shedding in pharyngeal secretions.

Active immunization

A number of groups are working on vaccines using inactivated SARS-CoV, recombinant SARS-CoV proteins and subunits, viral-vector vaccines and recombinant DNA vaccines.

Inactivated vaccines

Several reports have shown that inactivation of SARS-CoV with formaldehyde, UV light, and β-propiolactone can induce virus-neutralizing antibodies in immunized animals (20)(21)(22)(23)(24). In fact, the first inactivated SARS-CoV vaccine is being tested in clinical trials in China. However, there are serious concerns about the safety of this inactivated vaccine, and there is concern that production workers are at risk of infection during handling of the concentrated live SARS-CoV. Incomplete virus inactivation may cause SARS outbreaks among vaccinated populations (25). Takasuka *et al.* (26) have immunized mice with UV-inactivated SARS-CoV with or without adjuvant, and have shown that UV-inactivated SARS-CoV elicits marked humoral immunity, producing sustained antibody secretion and the production of memory B cells. They have also shown that UV-inactivated virions induce regional lymph node T cell-proliferation and marked cytokine production (IL-2, IL-4, IL-5, IFN-γ and TNF-α) following re-stimulation *in vitro*. He *et al.* (21) have demonstrated that SARS-CoV inactivated by beta-propiolactone elicits high titers of antibodies capable of recognizing the S

protein in immunized mice and rabbits. They have also shown that mouse and rabbit antiserum significantly inhibits S protein-mediated virus entry, suggesting that inactivated SARS vaccines might induce potent neutralizing antibodies capable of preventing SARS-CoV entry. Several other groups have also suggested that inactivated SARS-CoV virions might be useful. Kong *et al.* (27) have evaluated immune responses following exposure to different combinations of priming and boosting with DNA, adenoviruses, as well as inactivated viral vaccines. The ability to boost gene-based vaccines with adjuvanted inactivated virus shows clear enhancement of the CD4 and antibody responses. CD8 responses are not similarly enhanced by boosting.

Protein and/or subunit vaccines

At the present time, SARS-CoV S glycoprotein and related fragments are thought to be good candidates for the development of recombinant vaccines (Fig.1)(17)(22)(28)(29)(30)(31)(32). The N-terminal region of SARS-CoV S protein (S1) contains a putative RBD that is responsible for cell attachment (11)(31). He *et al.* (21) have shown that a recombinant fusion protein containing a 193-amino acid RBD (residues 318-510) and a human IgG1 Fc fragment induces potent antibody responses in immunized rabbits. These antibodies recognize the RBD of the S1 domain and completely inhibit SARS-CoV infection at a serum dilution of 1:10,240. Rabbit antiserum has been shown to effectively block binding of S1 to ACE2. van den Brink *et al.* have shown that a human monoclonal antibody specific for the RBD of SARS-CoV strain FM1 can effectively bind to the RBDs of most SARS-CoV strains (33). This suggests that antibodies directed against the RBD of a SARS-CoV isolate might neutralize infection by a broad spectrum of SARS-CoV strains. Therefore, recombinant proteins containing RBD or vectors encoding RBD might be used as vaccines for preventing infection by SARS-CoV with distinct genotypes. Recently, Pogrebnyak *et al.* (34) have demonstrated successful expression of the N-terminal region of the SARS-CoV S1 protein in transgenic plants, sufficient to induce an antibody response in mice fed the transgenic material. Mice parenterally primed with this plant-derived antigen have been observed to develop an immune response following booster immunization. This method has a number of practical, economic, and safety advantages over conventional systems for the production and delivery of subunit vaccines.

Ho *et al.* (35), Mortola and Roy (36), and Huang *et al.* (37), have all reported the formation of virus-like particles (VLPs) following the expression of several structural proteins of SARS-CoV using a baculovirus expression system or plasmid transfection of mammalian cells. These findings further advance our understanding of the morphogenesis of SARS-CoV and enable the generation of safe, conformational mimetics of the SARS-CoV that may facilitate the development of vaccines.

Viral-vector vaccines

Gao *et al.* (38) have constructed recombinant forms of adenovirus expressing the SARS-CoV S protein S1 fragment, M protein, and N protein. Intramuscular vaccination with all three recombinant adenoviruses on days 0 and 28 induces broad, virus-specific immunity in rhesus macaques. In their research, six vaccinated macaques demonstrated antibody responses against S protein, as well as T-cell responses against N protein. SARS-CoV specific neutralizing antibodies are detected in blood samples from all vaccinated animals *in vitro*. Bisht *et al.* (29) have constructed recombinant forms of a highly attenuated modified vaccinia virus Ankara (MVA) containing a gene encoding full-length SARS-CoV S protein. Expression of S protein alone after intranasal or intramuscular injection of recombinant MVA raises neutralizing antibody titers. Furthermore, four weeks after a second immunization, challenge of vaccinated and control animals with SARS-CoV shows reduced titers of SARS-CoV in the respiratory tracts of vaccinated animals. SARS-CoV replication in naive mice is reduced upon transfer of serum from mice immunized with recombinant MVA to naive mice. These findings suggest that MVA-based vaccines are potentially useful in the fight against SARS. Our group has constructed a series of recombinant DIs, a highly attenuated vaccinia strain (39), expressing a gene encoding four structural proteins (E, M, N and S), expressed individually or simultaneously. These recombinant DIs elicit the production of SARS-CoV-specific serum IgG antibodies and T-cell responses in vaccinated mice following intranasal or subcutaneous administration. Mice that have been subcutaneously vaccinated with recombinant DIs expressing E, M, N and S proteins combined demonstrate the greatest titers of serum neutralizing IgG antibodies and marked protective immunity against SARS-CoV challenge in the absence of a mucosal IgA response. This indicates that the potent immune response elicited by subcutaneous injection of recombinant DIs expressing S in combination with other membrane components (E, M, and N), may be capable of preventing mucosal infection by SARS-CoV (40). On the other hand, Weingartl's group have found that ferrets (*Mustela putorius furo*) immunized with recombinant rMVA expressing SARS-CoV S protein develop more rapid and vigorous neutralizing antibody responses, compared to control animals following challenge with SARS-CoV. However, marked inflammatory responses in the liver are also observed, suggesting that vaccination with recombinant MVA expressing SARS-CoV S protein may induce hepatitis (41)(42). This information is extremely important for development of safe SARS vaccines. Irregardless, extra caution should be taken when human trials of SARS vaccines are initiated given the potential for liver damage as a result of immunization, as well as the potential for inadvertent viral infection. Bukreyev *et al.* have constructed a recombinant attenuated parainfluenza virus (PIV) expressing SARS-CoV S protein, and

have immunized monkeys with a single dose of this recombinant PIV administered via the respiratory tract. Neutralizing serum antibodies can be detected in all vaccinated animals. Following SARS-CoV challenge, viral shedding is observed in control animals but not vaccinated monkeys (30). These results suggest that a vector mucosal vaccine expressing SARS-CoV S protein alone might be highly effective as a single-dose vaccine against SARS. This same group of researchers have further investigated the contribution of each structural protein to protective immunity by expressing them both individually and in combination using a recombinant PIV vector (32). Immunization with recombinant PIV expressing S provides complete protection against SARS-CoV challenge in the lower respiratory tract and partial protection in the upper respiratory tract. This suggests that S protein is the only antigen capable of inducing the production of neutralizing antibodies and subsequent protection against SARS-CoV infection. Faber *et al.* (43) have constructed recombinant rabies viruses (RVs) expressing SARS-CoV N or S proteins, and have studied their immunogenicity in mice. A single inoculation with recombinant RV expressing SARS-CoV S protein induces a marked SARS-CoV-neutralizing antibody response. On the other hand, antibodies against SARS-CoV N protein are not observed following a single inoculation with SARS-CoV N protein-expressing recombinant RV, probably because a single inoculation with RV primarily induces antibodies against a surface G protein, and not against internal RV proteins.

DNA vaccines

Yang *et al.* (28) have shown that a DNA vaccine encoding the S glycoprotein of SARS-CoV induces T cell and neutralizing antibody responses, as well as protective immunity, in a mouse model. Alternative forms of S protein have been analyzed by DNA immunization. DNA expression vectors induce a robust immune response mediated by CD4 and CD8 cells. Furthermore, neutralizing antibodies are observed in mice vaccinated with DNA expression vectors encoding a form of S with a preserved transmembrane domain. Viral replication is reduced by more than six orders of magnitude in the lungs of mice vaccinated with S plasmid DNA expression vectors, and protection is mediated by a humoral, rather than a T-cell-dependent, immune mechanism. Wang *et al.* (44) have produced marked titers of neutralizing antibodies using DNA vaccines encoding full-length S protein or S protein segments in rabbits. They have demonstrated major and minor neutralizing epitopes within the S1 and S2 subunits, respectively. These findings suggest that DNA vaccines based on the S glycoprotein effectively induce immune responses leading to protective immunity against SARS in animal models.

Kim *et al.* (45) have shown that DNA vaccination with antigen linked to calreticulin dramatically enhances major histocompatibility complex class I presentation of linked antigen to CD8 T cells. Thus, they have employed this method to create effective DNA vaccines using SARS-CoV N protein as the target antigen. Vaccination with naked CRT/N DNA generates the most potent N-specific humoral and T-cell-mediated immune responses in vaccinated C57BL/6 mice, compared to all other DNA constructs tested. Mice vaccinated with calreticulin /N DNA have significantly reduced viral titers of N protein-expressing SARS-CoV following challenge with SARS-CoV. Zhu *et al.* (46) have shown that immunization of mice with N-based DNA vaccines leads to N-specific antibody production and CTL activity. Zhao *et al.* (47) have also performed DNA immunization with the full length N gene and have shown that the N protein of SARS-CoV is an important B cell immunogen and that it can elicit broad-based cellular immune responses. Jin *et al.* (48) have performed a DNA vaccine experiment using a chemical adjuvant to show that E, M, and N gene constructs can induce high levels of specific antibodies, T cell proliferation, and IFN-c and DTH responses, along with *in vivo* cytotoxic T cell activity specifically directed against SARS-CoV antigens. The most marked immune responses occur following immunization with constructs encoding the nucleocapsid protein. Okada *et al.* (49) have demonstrated that SARS (M) DNA and (N) DNA vaccines induce SARS-CoV-specific CTL activity and T cell proliferation in mouse models and humans *in vivo* using SCID-PBL/hu.

Conclusions

Convalescent serum can be used to prevent the spread of SARS, as demonstrated in Hong Kong in 2003 (14). However, the use of convalescent serum is limited to those with symptoms at present. Investigators have drawn on their experiences with animal coronavirus vaccines to examine a number of different strategies for vaccine generation, including the use of inactivated viruses, purified protein, DNA, viral vectors and virus-like particles. An inactivated vaccine has been developed over a very short time period, however, there are a number of concerns regarding the safety of this inactivated vaccine (25). S protein has been demonstrated to be essential for inducing neutralizing antibodies against SARS-CoV since vaccines based on S protein induce neutralizing antibody responses. The N protein of SARS-CoV is also a potential target antigen for vaccine development, in particular, to induce cellular immunity. To achieve maximal protective immunity, immunogens used to develop vaccines should resemble the pathogenic virus themselves and be non-pathogenic. Purified VLPs of SARS-CoV closely fit this criteria and thus, provide attractive candidates for the development of a SARS vaccine (35) (36)(37). Attenuated strains of SARS-CoV may also be used, however, there is

no report of such kind of studies until now. It is also important to develop means to test the efficacy of various vaccines, since animal models to do so are lacking at the moment. Although there have been no reports of SARS in 2004 and 2005, it is strongly felt that SARS-CoV persists in an unidentified animal reservoir, such that the resurgence of SARS is still a serious threat. Therefore, SARS vaccines capable of eliciting potent neutralizing antibody responses and subsequent protection against infection and transmission are still likely to be developed.

References

1. Peiris, J. S., Guan, Y. & Yuen, K. Y. (2004) *Nat Med* 10, S88-97.
2. Lee, N., Hui, D., Wu, A., Chan, P., Cameron, P., Joynt, G. M., Ahuja, A., Yung, M. Y., Leung, C. B., To, K. F., Lui, S. F., Szeto, C. C., Chung, S. & Sung, J. J. (2003) *N Engl J Med* 348, 1986-94.
3. Drosten, C., Gunther, S., Preiser, W., van der Werf, S., Brodt, H. R., Becker, S., Rabenau, H., Panning, M., Kolesnikova, L., Fouchier, R. A., Berger, A., Burguiere, A. M., Cinatl, J., Eickmann, M., Escriou, N., Grywna, K., Kramme, S., Manuguerra, J. C., Muller, S., Rickerts, V., Sturmer, M., Vieth, S., Klenk, H. D., Osterhaus, A. D., Schmitz, H. & Doerr, H. W. (2003) *N Engl J Med* 348, 1967-76.
4. Ksiazek, T. G., Erdman, D., Goldsmith, C. S., Zaki, S. R., Peret, T., Emery, S., Tong, S., Urbani, C., Comer, J. A., Lim, W., Rollin, P. E., Dowell, S. F., Ling, A. E., Humphrey, C. D., Shieh, W. J., Guarner, J., Paddock, C. D., Rota, P., Fields, B., DeRisi, J., Yang, J. Y., Cox, N., Hughes, J. M., LeDuc, J. W., Bellini, W. J. & Anderson, L. J. (2003) *N Engl J Med* 348, 1953-66.
5. Marra, M. A., Jones, S. J., Astell, C. R., Holt, R. A., Brooks-Wilson, A., Butterfield, Y. S., Khattra, J., Asano, J. K., Barber, S. A., Chan, S. Y., Cloutier, A., Coughlin, S. M., Freeman, D., Girn, N., Griffith, O. L., Leach, S. R., Mayo, M., McDonald, H., Montgomery, S. B., Pandoh, P. K., Petrescu, A. S., Robertson, A. G., Schein, J. E., Siddiqui, A., Smailus, D. E., Stott, J. M., Yang, G. S., Plummer, F., Andonov, A., Artsob, H., Bastien, N., Bernard, K., Booth, T. F., Bowness, D., Czub, M., Drebot, M., Fernando, L., Flick, R., Garbutt, M., Gray, M., Grolla, A., Jones, S., Feldmann, H., Meyers, A., Kabani, A., Li, Y., Normand, S., Stroher, U., Tipples, G. A., Tyler, S., Vogrig, R., Ward, D., Watson, B., Brunham, R. C., Krajden, M., Petric, M., Skowronski, D. M., Upton, C. & Roper, R. L. (2003) *Science* 300, 1399-404.
6. Rota, P. A., Oberste, M. S., Monroe, S. S., Nix, W. A., Campagnoli, R., Icenogle, J. P., Penaranda, S., Bankamp, B., Maher, K., Chen, M. H., Tong, S., Tamin, A., Lowe, L., Frace, M., DeRisi, J. L., Chen, Q., Wang, D., Erdman, D. D., Peret, T. C., Burns, C., Ksiazek, T. G., Rollin, P. E., Sanchez, A., Liffick, S., Holloway, B., Limor, J., McCaustland, K., Olsen-Rasmussen, M., Fouchier, R., Gunther, S., Osterhaus, A. D., Drosten, C., Pallansch, M. A., Anderson, L. J. & Bellini, W. J. (2003) *Science* 300, 1394-9.
7. Holmes, K. V. (2003) *J Clin Invest* 111, 1605-9.
8. Collins, A. R., Knobler, R. L., Powell, H. & Buchmeier, M. J. (1982) *Virology* 119, 358-71.

9. Li, W., Moore, M. J., Vasilieva, N., Sui, J., Wong, S. K., Berne, M. A., Somasundaran, M., Sullivan, J. L., Luzuriaga, K., Greenough, T. C., Choe, H. & Farzan, M. (2003) *Nature* 426, 450-4.
10. Dimitrov, D. S. (2003) *Cell* 115, 652-3.
11. Wong, S. K., Li, W., Moore, M. J., Choe, H. & Farzan, M. (2004) *J Biol Chem* 279, 3197-201.
12. Xiao, X., Chakraborti, S., Dimitrov, A. S., Gramatikoff, K. & Dimitrov, D. S. (2003) *Biochem Biophys Res Commun* 312, 1159-64.
13. Liu, S., Xiao, G., Chen, Y., He, Y., Niu, J., Escalante, C. R., Xiong, H., Farmar, J., Debnath, A. K., Tien, P. & Jiang, S. (2004) *Lancet* 363, 938-47.
14. Wong, V. W., Dai, D., Wu, A. K. & Sung, J. J. (2003) *Hong Kong Med J* 9, 199-201.
15. Subbarao, K., McAuliffe, J., Vogel, L., Fahle, G., Fischer, S., Tatti, K., Packard, M., Shieh, W. J., Zaki, S. & Murphy, B. (2004) *J Virol* 78, 3572-7.
16. Traggiai, E., Becker, S., Subbarao, K., Kolesnikova, L., Uematsu, Y., Gismondo, M. R., Murphy, B. R., Rappuoli, R. & Lanzavecchia, A. (2004) *Nat Med* 10, 871-5.
17. Sui, J., Li, W., Murakami, A., Tamin, A., Matthews, L. J., Wong, S. K., Moore, M. J., Tallarico, A. S., Olurinde, M., Choe, H., Anderson, L. J., Bellini, W. J., Farzan, M. & Marasco, W. A. (2004) *Proc Natl Acad Sci U S A* 101, 2536-41.
18. Sui, J., Li, W., Roberts, A., Matthews, L. J., Murakami, A., Vogel, L., Wong, S. K., Subbarao, K., Farzan, M. & Marasco, W. A. (2005) *J Virol* 79, 5900-6.
19. ter Meulen, J., Bakker, A. B., van den Brink, E. N., Weverling, G. J., Martina, B. E., Haagmans, B. L., Kuiken, T., de Kruif, J., Preiser, W., Spaan, W., Gelderblom, H. R., Goudsmit, J. & Osterhaus, A. D. (2004) *Lancet* 363, 2139-41.
20. Xiong, S., Wang, Y. F., Zhang, M. Y., Liu, X. J., Zhang, C. H., Liu, S. S., Qian, C. W., Li, J. X., Lu, J. H., Wan, Z. Y., Zheng, H. Y., Yan, X. G., Meng, M. J. & Fan, J. L. (2004) *Immunol Lett* 95, 139-43.
21. He, Y., Zhou, Y., Siddiqui, P. & Jiang, S. (2004) *Biochem Biophys Res Commun* 325, 445-52.
22. Zhang, H., Wang, G., Li, J., Nie, Y., Shi, X., Lian, G., Wang, W., Yin, X., Zhao, Y., Qu, X., Ding, M. & Deng, H. (2004) *J Virol* 78, 6938-45.
23. Chou, T. H., Wang, S., Sakhatskyy, P. V., Mboudjeka, I., Lawrence, J. M., Huang, S., Coley, S., Yang, B., Li, J., Zhu, Q. & Lu, S. (2005) *Virology* 334, 134-43.
24. Qu, D., Zheng, B., Yao, X., Guan, Y., Yuan, Z. H., Zhong, N. S., Lu, L. W., Xie, J. P. & Wen, Y. M. (2005) *Vaccine* 23, 924-31.
25. Marshall, E. & Enserink, M. (2004) *Science* 303, 944-6.
26. Takasuka, N., Fujii, H., Takahashi, Y., Kasai, M., Morikawa, S., Itamura, S., Ishii, K., Sakaguchi, M., Ohnishi, K., Ohshima, M., Hashimoto, S., Odagiri, T., Tashiro, M., Yoshikura, H., Takemori, T. & Tsunetsugu-Yokota, Y. (2004) *Int Immunol* 16, 1423-30.
27. Kong, W. P., Xu, L., Stadler, K., Ulmer, J. B., Abrignani, S., Rappuoli, R. & Nabel, G. J. (2005) *J Virol* 79, 13915-23.
28. Yang, Z. Y., Kong, W. P., Huang, Y., Roberts, A., Murphy, B. R., Subbarao, K. & Nabel, G. J. (2004) *Nature* 428, 561-4.
29. Bisht, H., Roberts, A., Vogel, L., Bukreyev, A., Collins, P. L., Murphy, B. R., Subbarao, K. & Moss, B. (2004) *Proc Natl Acad Sci U S A* 101, 6641-6.